MULTI-AREA POWER SYSTEM STATE ESTIMATION UTILIZING BOUNDARY MEASUREMENTS AND PHASOR MEASUREMENT UNITS (PMUs)

A Thesis

by

MATTHEW A. FREEMAN

Submitted to the Office of Graduate Studies of
Texas A&M University
in partial fulfillment of the requirements for the degree of

MASTER OF SCIENCE

August 2006

Major Subject: Electrical Engineering

MULTI-AREA POWER SYSTEM STATE ESTIMATION UTILIZING BOUNDARY MEASUREMENTS AND PHASOR MEASUREMENT UNITS (PMUs)

A Thesis

by

MATTHEW A. FREEMAN

Submitted to the Office of Graduate Studies of
Texas A&M University
in partial fulfillment of the requirements for the degree of

MASTER OF SCIENCE

Approved by:

Chair of Committee,	Ali Abur
Committee Members,	Garng Huang
	Chanan Singh
	Salih Yurttas
Head of Department,	Steven Miller

August 2006

Major Subject: Electrical Engineering

ABSTRACT

Multi-Area Power System State Estimation Utilizing Boundary

Measurements and Phasor Measurement Units (PMUs). (August 2006)

Matthew A. Freeman, B.S., Texas A&M University

Chair of Advisory Committee: Dr. Ali Abur

The objective of this thesis is to prove the validity of a multi-area state estimator and investigate the advantages it provides over a serial state estimator. This is done utilizing the IEEE 118 Bus Test System as a sample system.

This thesis investigates the benefits that stem from utilizing a multi-area state estimator instead of a serial state estimator. These benefits are largely in the form of increased accuracy and decreased processing time. First, the theory behind power system state estimation is explained for a simple serial estimator. Then the thesis shows how conventional measurements and newer, more accurate PMU measurements work within the framework of weighted least squares estimation. Next, the multi-area state estimator is examined closely and the additional measurements provided by PMUs are used to increase accuracy and computational efficiency. Finally, the multi-area state estimator is tested for accuracy, its ability to detect bad data, and computation time.

ACKNOWLEDGMENTS

First of all, I would like to express my deepest gratitude to Dr. Abur, who has guided me throughout my undergraduate and graduate career. He has endured countless emails and confused looks, but never expressed anything but confidence in me and my ability as a scholar and a person.

Secondly, I would like to thank the members of my advisory committee, Dr. Garng Huang, Dr. Chanan Singh, and Dr. Salih Yurttas for all of their help and instruction throughout my time at Texas A&M.

I would also like to thank the Power Engineering Research Center for sponsoring my work which was part of this thesis.

Finally, I'd like to thank my family and friends for always being there when I needed them, no matter what.

TABLE OF CONTENTS

LIST OF FIGURES

LIST OF TABLES

CHAPTER I

INTRODUCTION

1.1 Modern Power Systems

The society that we live in depends on electricity. Electricity allows for instant communication across the globe, climatizes our buildings, and has let us extend our life span by more than 40 years [1]. It is the job of the power system engineers to ensure that this electricity is ready and available whenever it is required. These engineers have many tools at their disposal, and use everything from load forecasting to state estimation to ensure there is power at the flick of a switch.

Recently though, the power grid has become deregulated. In place of a large block of generators, transformers, and transmission lines owned and operated by a single company, there exists now a slapdash amalgamation of smaller companies each filling their own niche. This segmentation of the power grid has made the power system engineer's job much more complex. To complete the state estimation of the power grid, information must be gathered from many smaller, and often competing, companies. These companies may also utilize different algorithms and standards for their state estimators, and may feel reluctant to share this information with their competitors. These facts coupled with the massive size of the modern power system

---

This thesis follows the style and format of *IEEE Transactions on Power Systems.*

has made time efficient, numerically accurate state estimation difficult.

1.2 Multi-Area State Estimation

A new trend power system state estimation has emerged to combat these difficulties. This new approach, known as parallel or multi-area state estimation, involves breaking the problem down into two steps. The first step produces only the solution for subsystems, or individual areas, within the power grid. Once complete, the data from the individual areas feeds into the second step to create a single coordinated solution for the entire power system. This multi-area approach has been addressed in [2]-[3].

This thesis will demonstrate by example and simulation such an approach when applied to a sample power system. The IEEE 118 Bus Test System, divided into five different areas, shall serve as the sample system. The results produced by the multi-area state estimator will be compared with those of a standard single level, or serial state estimator and checked for accuracy, bad data detection, and time savings.

The particular algorithm used in this thesis was developed in [4]. In addition to conventional measurements such as bus power injections, line power flows, bus voltage and line current magnitudes, it also relies on the use of synchronized phasor measurement units (PMUs). These measurements allow for both the magnitude as well as the phase angle of bus voltages to be observed synchronized in time via the

Global Positioning System (GPS) technology. In this thesis, we will consider the use of few PMUs as measurement devices in different areas in order to facilitate synchronization of area slack bus voltage estimates.

1.3 Thesis Contribution

The contribution of this thesis will primarily be the application of a multi-area state estimation algorithm to sample power system. The multi-area technique will be explained and demonstrated on the IEEE 118 bus test system.

1.4 Thesis Organization

This thesis is organized into five chapters. In Chapter I, the current state of state estimation will be presented along with its challenges and some proposed solutions. Chapter II will deal with the nature of the state estimation problem and an algorithm will be developed taking into account the types of measurements, conventional or PMU, the issues involved with bad data and observability, and issues which appear with a multi-area approach. Chapter III will go deeper into the multi area solution and an algorithm will be developed and will address the issues raised in Chapter II. Chapter IV will present the results of this algorithm when applied to the IEEE sample system. Chapter V will summarize this thesis and point out work that still needs to be done in this field.

CHAPTER II

SERIAL STATE ESTIMATION

2.1 Weighted Least Squares Estimation

Simply put, state estimation is a technique used to capture the real-time operating conditions, or system states, of a power system. This technique has been extensively documented in [5]-[7]. In a system of N busses, there will be $(2N-1)$ system states. This will account for a voltage magnitude state variable at every bus and a voltage angle state variable at every bus but one. The uncounted bus angle is assumed to be zero and the bus is considered the reference, or slack bus of the system. The state vector will be organized such that the voltage magnitudes will be listed first, followed by the voltage phase angles as shown below.

$$x = \begin{pmatrix} |V_1| & |V_2| & \cdots & |V_N| & \theta_2 & \theta_3 & \cdots & \theta_N \end{pmatrix}$$

The state estimator takes the measurements received from the power system and uses them to estimate the system states. As it is an estimate, there will be some nominal errors associated with each measurement. This mathematical relationship is expressed below.

$$z = h(x) + e$$

$$\begin{bmatrix} z_1 \\ z_2 \\ \vdots \\ z_m \end{bmatrix} = \begin{bmatrix} h_1(x_1, x_2, \cdots, x_n) \\ h_2(x_1, x_2, \cdots, x_n) \\ \vdots \\ h_n(x_1, x_2, \cdots, x_n) \end{bmatrix} + \begin{bmatrix} e_1 \\ e_2 \\ \vdots \\ e_m \end{bmatrix}$$

$z^T = [z_1, z_2, \cdots, z_m]$	is the measurement vector
$h^T = [h_1(x), h_2(x), \cdots, h_n(x)]$	is the non-linear function relating the states to the measurements
$e^T = [e_1, e_2, \cdots, e_m]$	is the measurement error vector

The errors are assumed to be independent and uncorrelated with a zero mean. Furthermore, they are assumed to have a Gaussian (Normal) distribution. The covariance matrix associated with the errors will be a diagonal matrix R with the variance of the measurements as its entries.

$$E\{e_i\} = 0 \qquad i = 1,2,\cdots,m$$

$$E\{e_i e_j\} = 0 \qquad i = 1,2,\cdots,m \qquad j = 1,2,\cdots,m \qquad i \neq j$$

$$Cov(e) = E\{e \cdot e^T\} = R = diag\{\sigma_1^2, \sigma_2^2, \cdots, \sigma_m^2\}$$

In this thesis, weighted least squares (WLS) estimation will be applied to the above equations in order to extract the state quantities, bus voltages and angles, from the

measured values, power flows, injections and PMU measurements. WLS estimation seeks to minimize the weighted sum of the squares of the measurement errors.

This minimization will occur when the following objective function is minimized.

$$J(x) = \sum_{i=1}^{m} \left(z_i - h_i(x)\right)^2 \Big/ R_{ii} = \left[z - h(x)\right]^T R^{-1} \left[z - h(x)\right]$$

To minimize the above function, we simply set its first derivative with respect to x equal to zero, as shown below.

$$g(x) = \frac{\partial J(x)}{\partial x} = -\left[H(x)\right]^T \cdot R^{-1} \cdot \left[z - h(x)\right] = 0$$

$$H(x) = \frac{\partial h(x)}{\partial x}$$

We can apply the Gauss-Newton method to solve the above equation as shown below.

$$x_{k+1} = x_k - \left[G(x_k)\right]^{-1} \cdot g(x_k)$$

Above, k is the iteration index and x_k is the state vector at iteration k. The matrix $G(x)$ is called the gain matrix and is shown below.

$$G(x_k) = \frac{\partial g(x_k)}{\partial x} = [H(x_k)]^T \cdot R^{-1} \cdot H(x_k)$$

$$g(x_k) = -[H(x_k)]^T \cdot R^{-1} \cdot [z - h(x_k)]$$

The gain matrix is typically rather sparse and decomposed into its triangular factors. For every iteration, forward and backward substitutions are used to solve the following linear equations.

$$[G(x_k)]\Delta x_{k+1} = [H(x)]^T \cdot R^{-1} \cdot [z - h(x_k)] = [H(x_k)]^T \cdot R^{-1} \cdot \Delta z_k$$

$$\Delta x_{k+1} = x_{k+1} - x_k$$

These iterations will continue until one of two conditions are met. The first condition would be the maximum number of allowable iterations is exceeded while the second condition would be that the change in state variables has fallen within an acceptable range.

$$\max|\Delta x_k| < \varepsilon$$

A popular initial condition for state estimation is the flat start. This condition sets the voltages of all the busses equal to 1 p.u. with no phase change among the busses.

2.2 Treatment of Conventional Measurements

The five types of conventional measurements used in power system state estimation are real and reactive line power flows, real and reactive bus power injections, and the bus voltage magnitudes. In order to use these measurements in the state estimator, we must first develop a mathematical model for the measurements. To do this, consider the pi model of a transmission line which connects two busses i and j, as shown in Figure 1. The series admittance between bus i and j will be defined as $g_{ij} + jb_{ij}$ while the shunt admittance between any particular bus x and the ground will be defined as $g_{sx} + jb_{sx}$. The admittance matrix Y will be composed of $i \cdot j$ entries, with the entry $Y_{ij} = G_{ij} + jB_{ij}$.

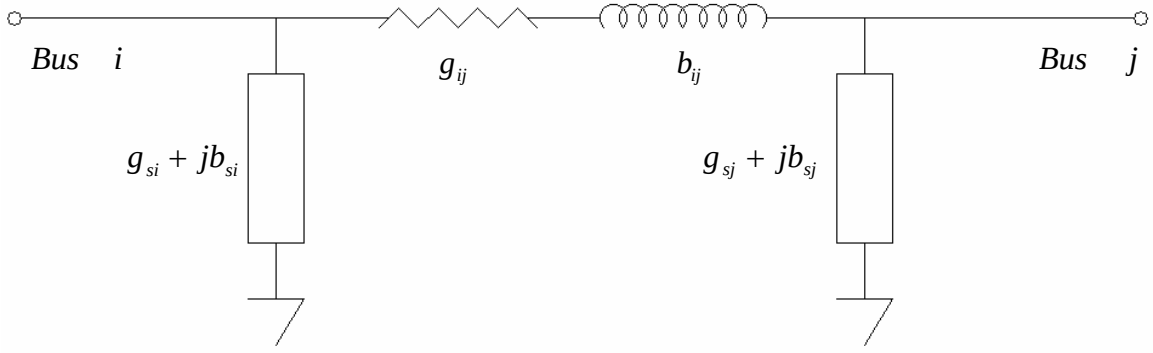

Figure 1. Conventional Measurement Transmission Line Model

Developing the equations for the power injection at bus i yields:

$$P_i = |V_i| \sum_{j \in N_i}^{N} |V_j| \left(G_{ij} \cos\theta_{ij} + B_{ij} \sin\theta_{ij} \right)$$

$$Q_i = |V_i| \sum_{j \in N_i}^{N} |V_j| \left(G_{ij} \sin\theta_{ij} - B_{ij} \cos\theta_{ij} \right)$$

For a real power injection, the Jacobian matrix components are shown below.

$$\frac{\partial P_i}{\partial |V_i|} = \sum_{j=1}^{N} |V_j| \left(G_{ij} \cos\theta_{ij} + B_{ij} \sin\theta_{ij} \right) - |V_i|^2 G_{ii}$$

$$\frac{\partial P_i}{\partial |V_j|} = |V_i| \left(G_{ij} \cos\theta_{ij} + B_{ij} \sin\theta_{ij} \right)$$

$$\frac{\partial P_i}{\partial \theta_i} = \sum_{j=1}^{N} |V_i| |V_j| \left(- G_{ij} \sin\theta_{ij} + B_{ij} \cos\theta_{ij} \right) - |V_i|^2 B_{ii}$$

$$\frac{\partial P_i}{\partial \theta_j} = |V_i| |V_j| \left(G_{ij} \sin\theta_{ij} - B_{ij} \cos\theta_{ij} \right)$$

For a reactive power injection, the H matrix components would take the following form.

$$\frac{\partial Q_i}{\partial |V_i|} = \sum_{j=1}^{N} |V_j| \left(G_{ij} \sin\theta_{ij} - B_{ij} \cos\theta_{ij} \right) - |V_i|^2 B_{ii}$$

$$\frac{\partial Q_i}{\partial |V_j|} = |V_i| \left(G_{ij} \sin\theta_{ij} - B_{ij} \cos\theta_{ij} \right)$$

$$\frac{\partial Q_i}{\partial \theta_i} = \sum_{j=1}^{N} |V_i| |V_j| \left(G_{ij} \cos\theta_{ij} + B_{ij} \sin\theta_{ij} \right) - |V_i|^2 G_{ii}$$

$$\frac{\partial Q_i}{\partial \theta_j} = |V_i| |V_j| \left(- G_{ij} \sin\theta_{ij} - B_{ij} \sin\theta_{ij} \right)$$

Similarly, the real and reactive power flows between busses *i* and *j* can be represented in the terms of the state variables in the following manner.

$$P_{ij} = |V_i|^2 \cdot \left(g_{si} + g_{ij} \right) - |V_i| \cdot |V_j| \cdot \left(g_{ij} \cos\theta_{ij} + b_{ij} \sin\theta_{ij} \right)$$

$$Q_{ij} = -|V_i|^2 \cdot \left(b_{si} + b_{ij} \right) - |V_i| \cdot |V_j| \cdot \left(g_{ij} \sin\theta_{ij} - b_{ij} \cos\theta_{ij} \right)$$

For a real power flow, the Jacobian matrix components are shown below.

$$\frac{\partial P_{ij}}{\partial |V_i|} = -|V_j|\left(-g_{ij}\cos\theta_{ij} + b_{ij}\sin\theta_{ij}\right) + 2|V_i|\left(g_{ij} + g_{si}\right)$$

$$\frac{\partial P_{ij}}{\partial |V_j|} = -|V_i|\left(g_{ij}\cos\theta_{ij} + b_{ij}\sin\theta_{ij}\right)$$

$$\frac{\partial P_{ij}}{\partial \theta_i} = |V_i||V_j|\left(g_{ij}\sin\theta_{ij} - b_{ij}\cos\theta_{ij}\right)$$

$$\frac{\partial P_{ij}}{\partial \theta_j} = -|V_i||V_j|\left(g_{ij}\sin\theta_{ij} - b_{ij}\cos\theta_{ij}\right)$$

For a reactive power flow, the components take the following form.

$$\frac{\partial Q_{ij}}{\partial |V_i|} = -|V_j|\left(g_{ij}\sin\theta_{ij} - b_{ij}\cos\theta_{ij}\right) - 2|V_i|\left(b_{ij} + b_{si}\right)$$

$$\frac{\partial Q_{ij}}{\partial |V_j|} = -|V_i|\left(g_{ij}\sin\theta_{ij} - b_{ij}\cos\theta_{ij}\right)$$

$$\frac{\partial Q_{ij}}{\partial \theta_i} = -|V_i||V_j|\left(g_{ij}\cos\theta_{ij} + b_{ij}\sin\theta_{ij}\right)$$

2.3 Treatment of Phasor Measurement Units

Phasor Measurement Units (PMUs) have several advantages over conventional measurements. Whereas a conventional measurement only has the ability to measure

the magnitude of a voltage, PMUs have the ability to measure the magnitude and phase angle of the bus voltages and the line currents in a system. Additionally, these measurements are synchronized with respect to time through the use of the GPS network. Additionally, the PMU has a smaller measurement variance which leads to smaller errors in the estimated state and a quicker convergence.

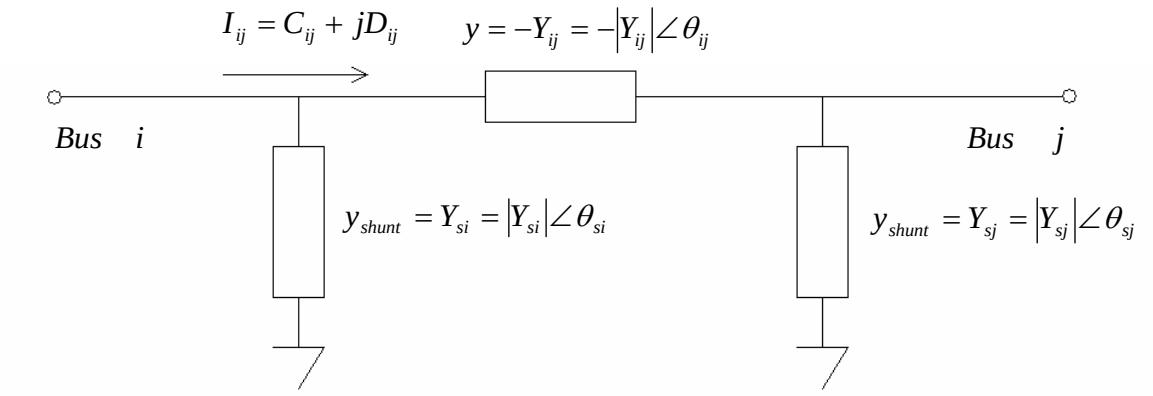

Figure 2. PMU Transmission Line Model

Consider the *pi* model of the transmission line connecting busses i and j shown Figure 2. This connection has a series admittance of y and a shunt admittance of shunt admittance of y_s. The equations describing the rectangular components of the complex current flowing through the branch can be derived as.

$$C_{ij} = |V_i Y_{si}|\cos(\delta_i + \theta_{si}) + |V_j Y_{ij}|\cos(\delta_j + \theta_{ij}) - |V_i Y_{ij}|\cos(\delta_i + \theta_{ij})$$

$$D_{ij} = |V_i Y_{si}|\sin(\delta_i + \theta_{si}) + |V_j Y_{ij}|\sin(\delta_j + \theta_{ij}) - |V_i Y_{ij}|\sin(\delta_i + \theta_{ij})$$

When the Jacobian H matrix is formed, the following derivatives of C_{ij} and D_{ij} are used.

$$\frac{\partial C_{ij}}{\partial V_i} = |Y_{si}|\cos(\delta_i + \theta_{si}) - |Y_{ij}|\cos(\delta_i + \theta_{ij})$$

$$\frac{\partial C_{ij}}{\partial V_j} = |Y_{ij}|\cos(\delta_j + \theta_{ij})$$

$$\frac{\partial C_{ij}}{\partial \delta_i} = -|V_i Y_{si}|\sin(\delta_i + \theta_{si}) + |V_i Y_{ij}|\sin(\delta_i + \theta_{ij})$$

$$\frac{\partial C_{ij}}{\partial \delta_j} = -|V_j Y_{ij}|\sin(\delta_j + \theta_{ij})$$

$$\frac{\partial D_{ij}}{\partial V_i} = |Y_{si}|\sin(\delta_i + \theta_{si}) - |Y_{ij}|\sin(\delta_i + \theta_{ij})$$

$$\frac{\partial D_{ij}}{\partial V_j} = |Y_{ij}|\sin(\delta_j + \theta_{ij})$$

$$\frac{\partial D_{ij}}{\partial \delta_i} = |V_i Y_{si}|\sin(\delta_i + \theta_{si}) - |V_i Y_{ij}|\cos(\delta_i + \theta_{ij})$$

$$\frac{\partial D_{ij}}{\partial \delta_j} = |V_j Y_{ij}|\cos(\delta_j + \theta_{ij})$$

When we employ PMUs in a power system, the measurement vector is augmented. Instead of containing only the voltage magnitude, power flows, and power injections provided by conventional measurements, it will also include the phase shifts and the real and reactive current flows throughout the system. The augmented measurement vector will take on the following form.

$$z = \begin{pmatrix} P_{inj}^T & Q_{inj}^T & P_{flo}^T & Q_{flo}^T & |V|^T & \delta^T & C_{ij}^T & D_{ij}^T \end{pmatrix}^T$$

2.4 Bad Data Processing

State estimators of all varieties are susceptible to the problem of bad data corruption. This bad data can come from many sources including a malfunctioning measurement device, a noisy communication channel, or even a failure in the communication channel. Whatever the source of the bad data, it will serve to bias the state estimator, causing it to return inaccurate results. One way of detecting the presence of bad data is using the χ^2 test. This test looks at the measurement vector z in an effort to determine the presence of faulty data. A second test involves the inspection of the normalized residuals to determine specifically which measurement is malfunctioning.

The χ^2 test may be looked at as having three separate steps. First, the state estimator must be run in order to obtain an estimate of the power systems state, $\hat{x}$. Once this state estimate has been calculated, the system's objective function must be developed. The objective function is of the following form.

$$J(x)=\sum_{i=1}^{m}\left(\frac{(z_i-h(x_i))^2}{R_{ii}}\right)=\sum_{i=1}^{m}R_{ii}^{-1}e_i^2$$

At this point, we can assume that all the error terms, e_i, will be random variables which are independent and approximately normally distributed in the following manner.

$$e_i=(z_i-h(\hat{x}_i))\sim N(0,R_{ii})$$

Now we are able to normalize the errors and obtain a new function $u(x)$.

$$u_i=\frac{z_i-h_i(x)}{\sqrt{R_{ii}}}$$

Once we have formulated the function $u(x)$, we enter the third part of the test. Now we must compute the χ^2 test statistic with $(m-n)$ degrees of freedom, where m is

the total number of measurements in the system and n is the number of states of the system. The false alarm rate α is then selected and a χ^2 table is consulted. If the value of the objective function $J(\hat{x})$ is greater than the χ^2 value, then we should suspect to have at least one piece of bad data in our measurement set. Should the value of the objective function be less than the χ^2 value, this is a good indication that all measurements are functioning properly.

There are two main shortcomings of this test. First of all, this is a cumulative test. This means that some of the outlying data points may be lost in the average, making this test less than perfect. Secondly, this test simply indicates the presence of bad data in our measurement set. The χ^2 test does not have the ability to single out the individual pieces of offending data, but merely says that they exist.

In order to find which specific measurement is incorrect, we must rely on another algorithm. This thesis will employ normalized residual testing in order to find the problematic measurements. In this technique, inspection of the normalized values of the residuals will point out which measurement is bad.

In order to use normalized residual testing, we must first define a matrix called the hat matrix, K.

$$K = HG^{-1}H^{T}R^{-1}$$

It is known as the hat matrix because the multiplication of K and Δz results in $\Delta\hat{z}$, in other words, the hat matrix simply puts a hat on Δz. With this K matrix, we are now able to develop the residual sensitivity matrix, S, in the following manner.

$$r = \Delta z - \Delta\hat{z} = \Delta z - K\Delta z$$

$$r = \Delta z(I - K)$$

$$r = (I - K)(H\Delta x + e)$$

$$r = H\Delta x - KH\Delta x + (I - K)e$$

$$r = (I - K)e = Se$$

Since the covariance matrix for e is assumed to be known as R, the above equation can be used to derive the covariance matrix for the residual vector r as follows:

$$r_i = z_i - h(\hat{x}_i)$$

$$Var(r) = SRS^{T}$$

It can be shown that SRS^T is equal to SR by substituting S with its expanded definition and simplifying terms. Hence:

$$Var(r_i) = SR_{ii} = \Omega_{ii}$$

$$r_i \sim N(0, \Omega_{ii})$$

We can normalize the residuals in the same manner that we normalized the errors to produce $u(x)$.

$$r_i^N = \frac{r_i}{\sqrt{\Omega_{ii}}}$$

$$r_i^N \sim N(0,1)$$

Now that the residual values have been normalized, they may be compared to some statistically reasonable value set by the observer based on the desired false alarm rate. A threshold of 3.0 is used in this thesis. Any residuals exceeding this threshold are suspect and should be treated.

The elimination of all bad data from a measurement set may be accomplished in the following manner. Once the normalized residuals have been calculated, the largest

residual will correspond to the erroneous measurement. Instead of removing this measurement from the vector, we are able to correct it using the following algorithm.

$$Z_i^{GOOD} = Z_i^{BAD} - \frac{\sigma_i^2}{\Omega_{ii}} r_i^{BAD}$$

$$r_i^{BAD} = Z_i^{BAD} - H\left(\hat{x}_i^{BAD}\right)$$

In the above equations, Z_i^{GOOD} and Z_i^{BAD} correspond to the corrected and initial, suspect value of the normalized residual for measurement i. By replacing Z_i^{BAD} with Z_i^{GOOD}, the bad data treatment algorithm is complete for the largest normalized residual of the group. The procedure may then be repeated until all normalized residuals fall beneath the threshold set by the user.

While this is a very useful technique for the discovery and elimination of bad data, it too has its shortfalls. This test has problems if the measurement scheme of the system is not robust. If there is a single piece of bad data, this algorithm will be unable to correct it if the faulty data is from a critical measurement. A critical measurement is a measurement which must be present in the system for the system to remain observable.

When there are multiple pieces of bad data, there are two issues. The first issue is concerned with the presence of a critical pair or k-tuple. These items are similar to critical measurements in the fact that if all the component measurements are removed, the system will become unobservable. There is also the issue of multiple interacting errors. Conforming interacting errors in particular pose a problem for this algorithm since it is possible for the conforming erroneous measurements to have smaller residuals than the measurements which are indeed free of gross errors.

This chapter has looked into the basics of weighted least squares state estimation as applied to electrical power systems. It has addressed the treatment of both conventional measurements and PMUs and given two tests for the detection and treatment of bad data. The next chapter will look at the process of multi-area state estimation.

CHAPTER III

MULTI-AREA STATE ESTIMATION

3.1 Introduction

As the electrical power networks of the world continue to grow ever larger, there has been an increasing demand for a highly robust, computationally efficient state estimation algorithm. Initially, this goal was pursued by taking advantage of the innately sparse structure of the state estimation matrices. New algorithms were developed to deal with large, sparse matrices and the state estimators kept pace with the power grids for a time. Unfortunately, the gains provided by sparse matrix manipulation were limited, and eventually the size of the power networks required a new advance in state estimation algorithms.

This new advance came in the form of parallel processing. Instead of being limited to a single serial processor, the parallel state estimators break the large system down into smaller sub-systems which are solved simultaneously on multiple processors. The state estimation results from these individual areas are then sent to a second coordinating processor where they are combined into a single solution for the entire system.

3.2 Multi-Area State Estimation

In any individual area in multi-area state estimation, there are three types of busses: internal, boundary, and external. Bus n of area i is considered to be internal if all of its neighboring busses also belong to area i. Bus n of area i is a boundary bus if at least one of its neighbors belongs to an area other than i. Finally, bus n will be an external bus of area i if it belongs to another area but has at least one connection to a boundary bus in area i. Any line running between two boundary busses of different areas, thus connecting the two areas, is known as a tie line. These four items are illustrated in the Figure 3 with busses 21, 22, and 23 being internal, boundary, and external busses to Area 1. There is a tie line running between busses 22 and 23 and another between 32 and 113.

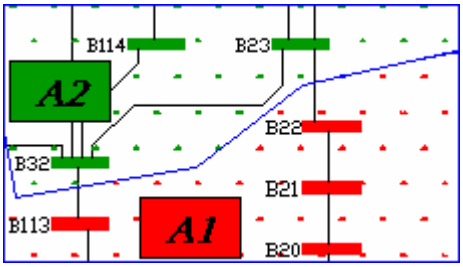

Figure 3. Multi-Area Bus Types

Since its inception, there have been many specific algorithms developed to carry out this parallel state estimation, some of the more successful ones have been detailed in [8]-[13]. In most cases, the first level state estimation is identical. The large system is

broken down into smaller, more manageable areas and the standard state estimation algorithm is applied, as was shown in Chapter II. There is a great deal of confusion though about what to do from that point. Most of this confusion concerns what to do with the boundary measurements. Some algorithms insert a non-existent bus in between the boundary busses on tie lines [14]. Other methods based on the work in [15] break the system down into non-overlapping systems and then apply the model coordination method to come to a solution. More recently though, the work done in [4] and [16] has developed the algorithm which will be used in this thesis.

In [16] the author first decomposes the system into a group of overlapping subsystems. This is accomplished by including the boundary busses and external busses in both areas which they are associated with. Once the first stage of state estimation is complete, the state vectors for each area are organized in the following manner.

$$x_i = \left[x_i^{b^T} \quad x_i^{\text{int}^T} \quad x_i^{ext^T} \right]$$

For each area i, the components of the state vector x_i are organized by bus type. In the equation above, $x_i^{b^T}$ is the state vector composed of the voltage magnitude and phase angles at the boundary busses, $x_i^{\text{int}^T}$ is the state vector composed of the voltage

magnitude and phase angles at the internal busses, and $x_i^{ext^T}$ is the state vector composed of the voltage magnitude and phase angles at the external busses. In each area, the phase angle of the slack bus will be removed from the appropriate vector.

Once this first stage is complete, the estimation coordination must begin. The coordinating estimator is not only responsible for the coordinating of the individual area results, but must also carry out bad data detection and correction for the boundary measurements. The states used in this coordinating estimator include not only the states computed for each individual area, but also include the synchronized voltage phasors for the slack bus in each area. This state vector is defined in the following manner.

$$x_s = \begin{bmatrix} x^{b^T} & u^T \end{bmatrix}^T$$

$$x^{b^T} = \begin{bmatrix} x_1^{b^T} & x_2^{b^T} & \cdots & x_n^{b^T} \end{bmatrix}^T$$

$$u^T = \begin{bmatrix} u_2 & u_3 & \cdots & u_n \end{bmatrix}^T$$

The voltage angle of the slack bus in each area measured with respect to the voltage angle of the slack bus in the first area is listed as u_i. The global reference bus among the individual area slack busses was chosen at random to be the slack bus in the first

area, and could easily be any of the slack busses in the system. In this case, the u^T vector would start with u_1 and exclude the appropriate entry containing the slack reference bus.

At the second level of state estimation, the coordinating estimator will utilize a measurement vector with the following composition.

$$z = \begin{bmatrix} z_u^T & z_{sp}^T & \hat{x}^{b^T} & \hat{x}^{ext^T} \end{bmatrix}^T$$

In the above measurement vector, z_u^T is the vector of boundary measurements, z_{sp}^T is the vector of synchronized phasor measurements, and $\hat{x}^{b^T}$ and $\hat{x}^{ext^T}$ are the vectors of boundary and external state variables as estimated by the individual areas. This vector of states will then be treated as pseudo-measurements by the coordinating estimator. This leads us to the measurement model which will be used by the second level state estimator shown below.

$$z_s = h_s(x_s) + e_s$$

The covariance of these estimated measurements are obtained from the covariance matrix of the area from which they come. This covariance matrix is actually the inverse of the gain matrix of the area, as shown below.

$$\operatorname{cov}(\hat{x}) = \operatorname{cov}\left(\left(H^T R^{-1} H^T\right)^{-1} H^T R^{-1} z\right)$$

$$\operatorname{cov}(\hat{x}) = \operatorname{cov}\left(G^{-1} H^T R^{-1} z\right)$$

$$\operatorname{cov}(\hat{x}) = \left(G^{-1} H^T R^{-1}\right)\operatorname{cov}(z)\left(G^{-1} H^T R^{-1}\right)^T$$

$$\operatorname{cov}(\hat{x}) = \left(G^{-1} H^T R^{-1}\right)R\left(\left(H^T R^{-1} H\right)^{-1} H^T R^{-1}\right)^T$$

$$\operatorname{cov}(\hat{x}) = \left(G^{-1} H^T R^{-1}\right)R\left(H^T R^{-1}\right)^T \left(\left(H^T R^{-1} H\right)^{-1}\right)^T$$

$$\operatorname{cov}(\hat{x}) = \left(G^{-1} H^T R^{-1}\right)RR^{-1} HH^{-1} R\left(H^T\right)^{-1}$$

$$\operatorname{cov}(\hat{x}) = G^{-1} H^T R^{-1} R\left(H^T\right)^{-1}$$

$$\operatorname{cov}(\hat{x}) = G^{-1}$$

Once the coordinating estimator has reached a WLS solution for the entire area, residual testing may then take place, and any faulty measurements will be

normalized. While this is an excellent procedure since it does not require the sharing of data between the areas, it can be improved upon still.

In [4], the author points out that the above technique simply uses the PMUs to measure the synchronized voltage angles among the areas and suggests the following. PMUs have the ability to measure the real and reactive current phasors. In fact, a single PMU may measure a bus voltage phasor and multiple current phasors simultaneously. As the measurements taken from PMUs have smaller variance than conventional measurements, the estimated state would benefit from the inclusion of these additional PMU current measurements.

The first level of state estimation with PMUs would follow the algorithm outlined in Chapter II. Once the states of the individual areas have been estimated though, the second level algorithm needs to be changed in order to accommodate the additional measurements provided by the PMUs. The new measurement vector of the second level state estimator will be of the following form.

$$z_s = \begin{bmatrix} z_u^T & z_{pmu}^T & \hat{x}^{b\,T} & \hat{x}^{ext\,T} \end{bmatrix}^T$$

$$z_{pmu} = \begin{bmatrix} z_{|v|}^T & z_\theta^T & z_C^T & z_D^T \end{bmatrix}^T$$

$$z_s = \begin{bmatrix} z_u^T & z_{|v|}^T & z_\theta^T & z_C^T & z_D^T & \hat{x}^{b^T} & \hat{x}^{ext^T} \end{bmatrix}^T$$

Above, z_{PMU} is the measurement vector from a PMU. The overall measurement vector, z_s, will contain twelve different types of measurements, four from conventional measurements, four from PMU measurements, and four pseudo-measurements from the first level of estimation. These twelve measurement types are detailed below.

Table 1. Multi-Area Measurement Types and Sources

Source	Measurement
Conventional	Real power flow
	Reactive power flow
	Real power injection
	Reactive power injection
PMU	Voltage magnitude
	Voltage phase angle
	Real Current
	Reactive Current
Estimated	Boundary bus voltage magnitude
	Boundary bus voltage phase angle
	External bus voltage magnitude
	External bus voltage phase angle

At this coordination level, the state vector contains the states from the boundary busses, as well as the states from the busses supporting a PMU and its neighboring busses.

$$x_s = \left[x^{b^T} \quad x_{pmu}^T \right]^T$$

Including this additional information does indeed increase the performance of the state estimator as shown in [4].

This chapter has laid out the basic theory behind multi-area state estimation, including the terminology, measurement types and measurement vector composition. In the following chapter, this algorithm will be tested and verified on the IEEE 118 bus test system. Its results shall not only be checked for accuracy with a standard state estimator, but its ability to detect bad data will also be put to the test.

CHAPTER IV

SIMULATION RESULTS

4.1 118 Bus Area Geography

Before the test system is fed into the estimator, it must first be broken down into individual areas. The division of these areas do not play an important role in the second level solution, so the formation of the areas is subject to only one stipulation, the individual areas must be observable. If an individual area is unobservable, the first level state estimator will be unable to converge for that area. This will lead to missing information for the second level estimator, again causing a non-converging error. I chose to break the system down into five areas. Table 2 details the bus composition of each area in the IEEE 118 bus test system. Figure 4 shows the IEEE 118 Bus Test System. In the system diagram, the slack busses for each area are shown in blue. The arrows branching off of the slack busses indicate a complex current measurement, provided by the PMU at that bus.

Table 2. 118 Bus System Area Composition

Area	*1*	*2*	*3*	*4*	*5*
Internal Busses	20	16	22	14	4
Boundary Busses	6	11	5	11	9
External Busses	7	9	6	10	13
Total Busses	26	27	27	25	13
Slack Bus No.	3	27	103	35	47

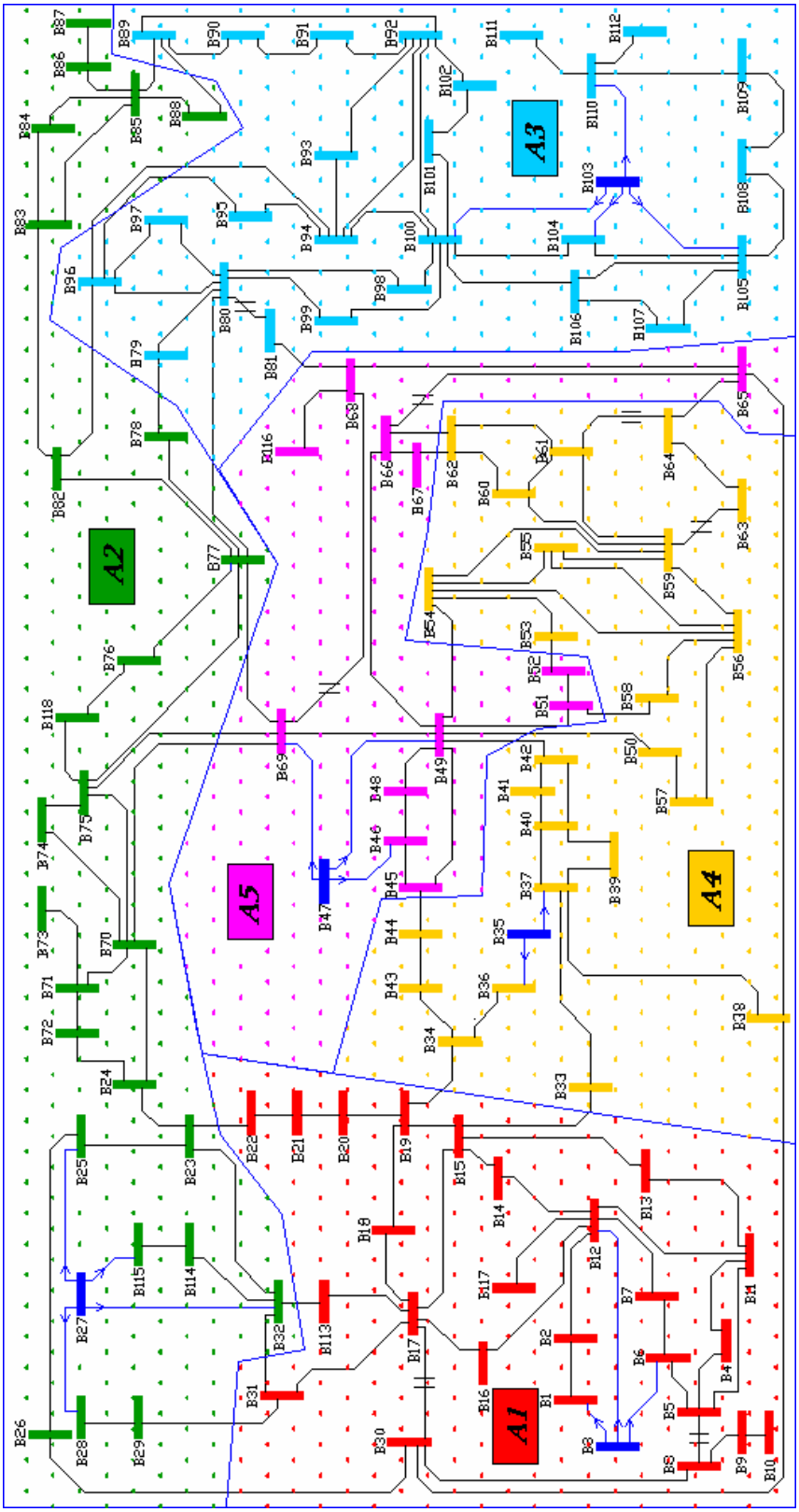

Figure 4. IEEE 118 Bus Test System

4.2 Measurement Vector Composition

In order to create the measurements used by the state estimators in this thesis, a power flow analysis was first run on the integrated system. The resulting currents and power flows were then perturbed by a small amount to simulate the variance found in actual measurements. The different types of measurements were subjected to different amounts of perturbation, as detailed in Table 3. Notice that the standard deviation of all the PMU measurements is significantly smaller than the standard deviation of the conventional measurements. This reflects the increased precision of the newer PMUs over the conventional measurement devices.

Table 3. Measurement Standard Deviation

Measurement Type	*Standard Deviation*
Conventional Power Injection	0.01
Conventional Power Flow	0.008
PMU Real Current	0.000001
PMU Reactive Current	0.000001
PMU Voltage Magnitude	0.000001
PMU Voltage Angle	0.000001

In the serial estimator and the individual area estimators, the boundary busses received a real and reactive power injection measurement pair. All branches received at least one real and reactive power flow measurement pair, and if the branch was associated with a boundary bus, it received a second real and reactive power flow

measurement pair. Finally, the slack busses in each area received a PMU voltage magnitude measurement.

For the multi-area estimator, the power injection measurement pairs were assigned in the same manner. At this level, only the branches associated with a boundary bus receive power flow measurement pairs, and these branches receive two measurement pairs. The slack bus within each area is given a voltage magnitude and angle measurement from the PMU located at that bus. Any boundary bus or external bus will receive a voltage magnitude and angle pseudo-measurement from the first level state estimation. Finally, the real and reactive current flows from the slack busses in each area was also included in the second level measurement vector. Table 4 summarizes the measurement make up of the various estimators.

Table 4. Measurement Vector Composition per Estimator

Estimator	*Serial*	*Individual Area*					*Multi-Area*
		1	*2*	*3*	*4*	*5*	
Injection Pairs	42	6	11	5	11	9	42
Flow Pairs	252	74	77	84	77	46	206
Slack Voltage Phasor	5	1	1	1	1	1	5
Boundary Voltage Phasor	0	0	0	0	0	0	42
External Voltage Phasor	0	0	0	0	0	0	42

4.3 Accuracy Verification

Now that we have defined our systems and measurement vectors, we are able to begin simulation. This first round of simulation will be simply to determine if the accuracy of the multi-area of the state estimator is on par with that of the serial estimator. Figures 5 and 6 show the voltage magnitude and angle difference between the given solution and the serial estimator, as well as the given solution and the multi-area estimator.

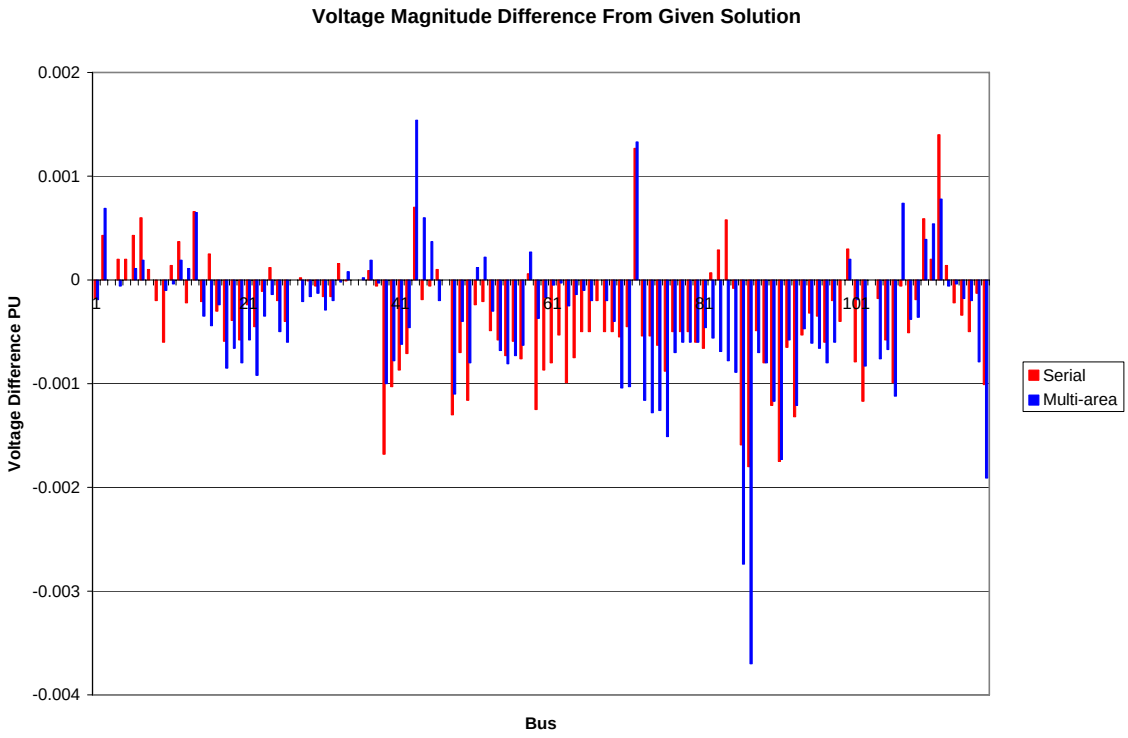

Figure 5. Voltage Magnitude Difference Comparison

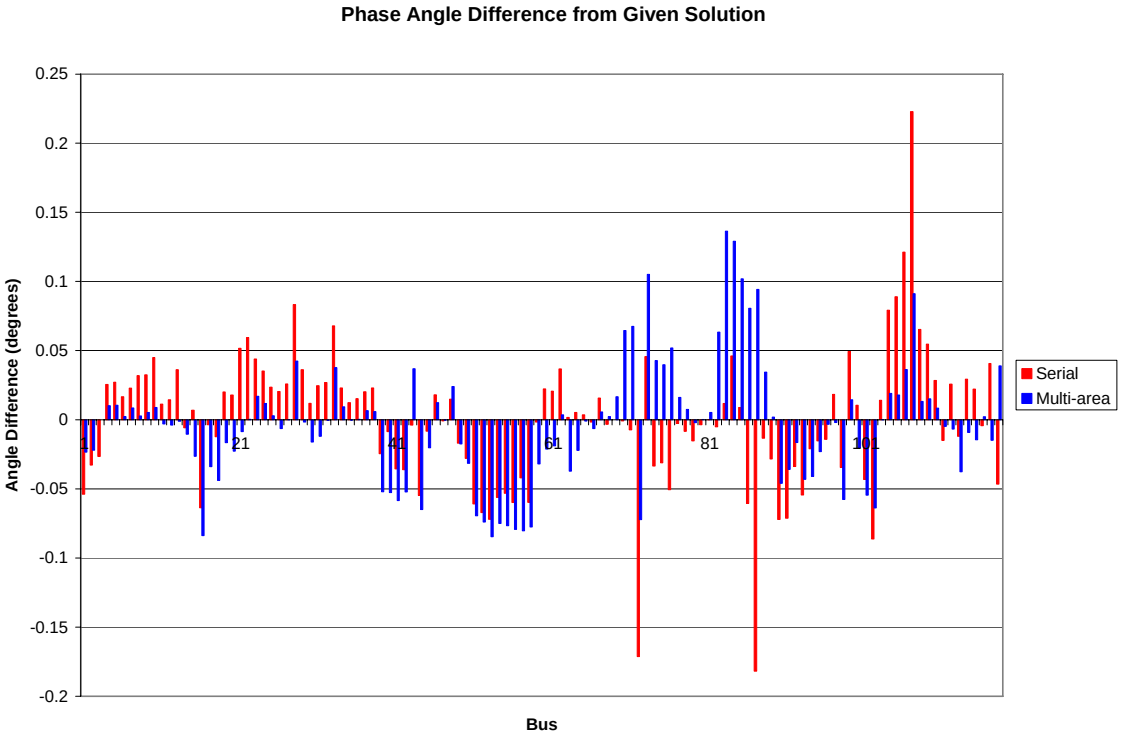

Figure 6. Phase Angle Difference Comparison

While Figures 5 and 6 may be a little confusing, their pertinent statistics are summarized in the Table 5 below.

Table 5. Estimator Accuracy Statistics

Estimator	*Serial Estimator*	*Multi-Area Estimator*
Mean Voltage Difference	-0.00033	-0.00038
Mean Angle Difference (°)	0.00004	-0.00362
Voltage Difference Standard Deviation	0.00055	0.00067
Angle Difference Standard Deviation (°)	0.04909	0.04318
Max Voltage Difference	0.0018	0.0037
Max Angle Difference (°)	0.22286	0.13645

It can be seen that the difference between the serial estimator and the multi-state estimator is minimal. This verifies that the multi-state estimator does function correctly given ideal conditions. The next step is to verify the multi-state estimator's ability to detect bad data.

4.4 Bad Data Detection

As pointed out in Chapter II, the state estimators use a χ^2 test to detect the presence of bad data and then an investigation of the normalized residual values will point out the specific measurement which is returning the bad data.

For the χ^2 test, the objective function of the system must be compared to a threshold value. This value is determined by setting a false alarm probability, α and the degrees of freedom for the system, given by $(m-(2N-1))$, where m is the total number of measurements in the area and N is the number of busses in the area. When the value of any normalized residual exceeds 3.0, this indicates the measurement associated with that residual is returning bad data. Table 6 lays out the data and thresholds used for bad data detection with for the serial, individual area, and multi-area state estimators.

Table 6. Bad Data Detection per Estimator

Estimator	*Serial*	*Individual Area*					*Multi-Area*
		1	*2*	*3*	*4*	*5*	
Measurements	593	161	177	179	177	111	680
Busses	118	26	27	27	25	13	118
Degrees of Freedom	356	108	122	124	126	84	443
False Alarm Rate	0.01	0.01	0.01	0.01	0.01	0.01	0.01
Chi-squared Value	421.00	145.10	161.25	163.55	165.84	117.06	515.17
Objective Function	348.43	93.22	105.99	112.17	126.08	57.41	481.69
Largest Normalized Residual	0.301	0.278	0.242	0.250	0.281	0.276	0.403

As can be seen above, the largest normalized residuals for each of the estimators is well below the 3.0 threshold, indicating all the data is within reason. This fact is further confirmed since the objective function of each of the areas is well below the chi-squared value as determined by the degrees of freedom and the false alarm rate.

To test the multi-area estimator's ability to detect bad data, let us force a bad power injection measurement at Bus 19 in Area 1. By changing the computed measurement value from -0.46304 to -1, we will be able to see if the estimators are able to first detect and then isolate the bad data using both the χ^2 and normalized residual tests.

Table 7 shows the results of this faulty measurement on the test statistics of the system.

Table 7. Bad Data Detected per Estimator

Estimator	*Serial*	*Individual Area*					*Multi-Area*
		1	*2*	*3*	*4*	*5*	
Chi-squared Value	421.00	145.10	161.25	163.55	165.84	117.06	515.17
Objective Function	1575.90	1233.20	126.38	109.30	98.92	48.62	1935.50
Largest Normalized Residual	3.512	3.381	0.295	0.275	0.312	0.253	3.650

It can be seen that the multi-area estimator does indeed have the ability to detect bad data. This is evident in the fact that the objective function of the system is greater than the chi-squared test statistic. The only measurement residual which was larger than the allowed threshold of 3.0 was the residual which corresponded to the power injection measurement at Bus 19.

4.5 CPU Time Savings

Now that this thesis has shown the multi-area state estimator to be accurate and robust, we are able to examine the possible time savings which come from a parallel processing scheme. The large scale of modern utility power systems were a driving force behind the development of multi-area state estimators. Unfortunately, any time savings seen on the IEEE 118 Bus Test System will be minimal at best due to its small size, but the time savings will increase as the systems grow larger.

In order to determine the time savings offered by the multi-area state estimator, the CPU clock will first record the time required for the serial state estimator to converge. Then, the CPU clock will record the time required for each of the individual area state estimators to converge. Of these five times, the longest time will be added to the time required for the coordination level state estimator to converge. The CPU clock will begin timing at the start of the state estimation algorithm and will stop once the largest normalized residual has been calculated. This removes any extraneous cycles required for reading in data files or calculating measurements which may skew the results. Table 8 holds the various times taken by each of the estimators.

Table 8. Time Savings of Multi-Area Estimation

Estimator	*Base Time*	*Total Time*
Serial	0.7711	0.7711
Area 1	0.2403	0.9814
Area 2	0.1803	
Area 3	0.1702	
Area 4	0.1502	
Area 5	0.1001	
Multi Area	0.7411	

Unfortunately, on such a small scale the time savings of running a multi-area state estimator are not apparent. When dealing with utility power systems which contain thousands of busses and branches, one could expect a very real time savings.

This chapter has shown that the accuracy of the multi-area state estimator is on par with that of a standard state estimator. The multi-area state estimator also is able to use the same tests as a serial estimator to detect bad data received from its measurements. Finally, an attempt was made to examine the time savings of multi-area state estimation, but the scale of the system was too small for a determination to be made.

CHAPTER V

CONCLUSION

5.1 Summary

Chapter II was a study in the theory of power system state estimation. The objective of state estimation is to describe the real time operation of a power system in terms of the systems states, bus voltage magnitude and phase angle. To do this, the state estimator relies on various measurements taken from the power system, including power injections, power flows, and PMU measurements. The power system measurements were modeled as the sum of a non-linear function relating the error measurements to the system states and a random variable representing error. Weighted least squares estimation was then used to minimize the sum of the square of the error. The mathematical equations related to the use of conventional and PMU measurements in WLS estimation were derived and examined. Finally, the issue of bad data processing was explored. There were two types of bad data treatments used in this thesis. The chi-squared test was the first method and is only used to tell if there is at least one bad measurement in the measurement vector. In order to determine which specific measurement is bad, one needs to use the normalized residual test.

Chapter III took the state estimation algorithm developed in Chapter II and attempted to make it faster. To do this, the idea of a multi-area state estimator was discussed. In a multi-area state estimator, the single large power system is broken down into smaller areas. These individual areas each run their own state estimation algorithm simultaneously and then pass the results to a second level coordinating estimator. This second level estimation pieces the information from the first level to create a single state vector for the entire system. The use of PMUs is vital at this coordination level, and the use of their measurements was discussed.

Chapter IV was simply a verification of the validity of the multi-area state estimator developed in Chapter III. In order to verify the accuracy of multi-area state estimator, the IEEE 118 Bus Test System was first run through a serial state estimator. This state vector and the state vector given as the solution were used as a baseline to compare the performance of the multi-area state estimator. Then the IEEE 118 Bus Test System was broken down into five areas in preparation for the multi-area state estimator. The measurement scheme of the multi-area state estimator was once again explained, and then the multi-area state vector was compared to the baseline. It was shown that the performance of the multi-area state estimator was comparable to the performance of the serial state estimator in terms of accuracy. The next test was to see if the multi-area state estimator would be able to detect bad measurement data. This was done by perturbing the measurement vector and in every case, the multi-

area state estimator detected the bad data with both the χ^2 test and the normalized residual test. Finally, the time savings stemming from the use of the multi-area state estimator were investigated. Unfortunately, the size of the test system was such that the gains were unobservable.

5.2 Future Work

While this thesis was successful in verifying the accuracy of the multi-area state estimator, it was unable to see any time savings due to the implementation of said estimator. It has been said many times throughout this thesis that the shortened computation time was the impetus for the development of multi-area state estimation, and as such, this deserves further study. The next logical step would be to increase the size of the system and look for the promised reduction in computation time.

REFERENCES

[1] J. Oeppen, J.Vaupel, "Broken Limits to Life Expectancy," *SCIENCE*, vol. 296, pp. 1030-1031, May 2002.

[2] D.M. Falcao, F.F. Wu, L. Murphy, "Parallel and Distributed State Estimation," *IEEE Transactions on Power Systems*, vol. 10, no. 2, pp. 724-730, May 1995.

[3] J.B. Carvalho, F.M. Barbosa, "Parallel and Distributed Processing State Estimation of Power System Energy," *9th Mediterranean Electrotechnical Conference*, vol. 2, pp. 969-973, May 1998.

[4] Yeojun Yoon, "Study of the Utilization and Benefits of Phasor Measurement Units for Large Scale Power System State Estimation," MS Thesis, Texas A&M University, Dec 2005.

[5] A. Bose, K.A. Clements, "Real-Time Modeling of Power Networks," *in Proc. of the IEEE*, vol. 75, no. 12, pp. 1607-1622, December 1987.

[6] A. Abur, A.G. Exposito, *Power System State Estimation: Theory and Implementation*, New York, Marcel Dekker, 2004.

[7] F.C. Schweppe, J. Wildes, D.B. Rom, "Power System Static State Estimation I, II, III," *IEEE Transactions on PAS*, vol. PAS-89, no. 1, pp. 120-135, January 1970.

[8] D.P. Bertsekas, J.N. Tsitsikilis, *Parallel and Distributed Computation*, Upper Saddle River, New Jersey, Prentice Hall, 1989.

[9] F.F. Wu, "Parallel Processing in Power Systems Computation," *IEEE Transactions on Power Systems*, vol. 7, no 2, pp. 629-638, August 1992.

[10] D.J. Tylavsky, A. Bose, F. Alvarado, R. Betancourt, K. Clements et al, "Parallel Processing in Power Systems Computation," *IEEE Transactions on Power Systems*, vol. 7, no. 2, pp. 629-638, May 1992.

[11] K. Hwang, F. Briggs, *Computer Architecture and Parallel Processing*, New York, McGraw-Hill, 1984.

[12] A.A. El-Keib, C.C. Carroll, H. Singh, D.J. Maratukulam, "Parallel State Estimation in Power Systems," *Twenty-Second Southeastern Symposium on System Theory*, Cookeville, Tennessee, March 1990, pp. 255-260.

[13] T. Van Cutsem, M. Ribbens-Pavella, "Critical Survey of Hierarchical Methods for State Estimation of Electric Power Systems,' *IEEE Transactions on PAS*, vol. PAS-102, no. 10, pp 3415-3424, October 1983.

[14] J.B. Carvalho, F.M. Barbosa, "A Parallel Algorithm to Power Systems State Estimation," *1998 International Conference on Power System Technology*, vol. 2, pp. 1213-1217, August 1998.

[15] H. Kobayashi, S. Narita, M.S.A.A. Hammam, "Model Coordination Method Applied to Power System Control and Estimation Problems," *in Proc. of the IFAC/IFIP 4th International Conference*, Santiago de Chile, 1974, pp. 291-298.

[16] L. Zhao, A. Abur, "Multi Area State Estimation Using Synchronized Phasor Measurements," *IEEE Transactions on Power Systems*, vol. 20, no. 2, pp. 611-617, May 2005.

VITA

Name:	Matthew Allan Freeman
Address:	560 22nd Street
	Beaumont, TX 77706
Email Address:	freeman.matt@gmail.com
Education:	B.S., Electrical Engineering, Texas A&M University, 2004
	M.S., Electrical Engineering, Texas A&M University, 2006